Published in final edited form as:
Hepatology. 2014 November ; 60(5): 1753–1766. doi:10.1002/hep.27285.

Antagonistic interaction between Wnt and Notch activity modulates the regenerative capacity of a zebrafish fibrotic liver model

Mianbo Huang[1], **Angela Chang**[1], **Minna Choi**[1], **David Zhou**[1], **Frank A. Anania**[2], and **Chong Hyun Shin**[1,*]

[1]School of Biology and the Parker H. Petit Institute for Bioengineering and Bioscience Georgia Institute of Technology, Atlanta, GA 30332, USA

[2]Division of Digestive Diseases, Emory University School of Medicine, Atlanta, GA 30322, USA

Abstract

In chronic liver failure patients with sustained fibrosis, excessive accumulation of extracellular matrix (ECM) proteins substantially dampens the regenerative capacity of the hepatocytes, resulting in poor prognosis and high mortality. Currently, the mechanisms and the strategies of inducing endogenous cellular sources such as hepatic progenitor cells (HPCs) to regenerate hepatocytes in various contexts of fibrogenic stimuli remain elusive. Here, we aim to understand the molecular and cellular mechanisms that mediate the effects of sustained fibrosis on hepatocyte regeneration using the zebrafish as a model. In the ethanol-induced fibrotic zebrafish model, we identified a subset of HPCs, responsive to Notch signaling, that retains its capacity to regenerate as hepatocytes. Discrete levels of Notch signaling modulate distinct cellular outcomes of these Notch responsive HPCs in hepatocyte regeneration. Lower levels of Notch signaling promote amplification and subsequent differentiation of these cells into hepatocytes, while high levels of Notch signaling suppress these processes. To identify small molecules facilitating hepatocyte regeneration in the fibrotic liver, we performed chemical screens and identified a number of Wnt agonists and Notch antagonists. Further analyses demonstrated that these Wnt agonists are capable of attenuating Notch signaling by inducing Numb, a membrane-associated protein that inhibits Notch signaling. This suggests that the antagonistic interplay between Wnt and Notch signaling crucially affects hepatocyte regeneration in the fibrotic liver.

Conclusion—Our findings not only elucidate how signaling pathways and cell-cell communications direct the cellular response of HPCs to fibrogenic stimuli, but also identify novel potential therapeutic strategies for chronic liver disease.

Keywords

Fibrosis; Hepatic progenitor cells; Hepatocytes; Notch-responsive cells; Regeneration

[*]To whom correspondence should be addressed: Chong Hyun Shin, Ph.D., School of Biology and the Parker H. Petit Institute for Bioengineering and Bioscience, Interdisciplinary Bioengineering Graduate Program, Georgia Institute of Technology, 315 Ferst Drive NW, Room 1313, Atlanta, GA 30332, USA, Chong.Shin@biology.gatech.edu, Telephone: 404-385-4211.

Sustained liver fibrosis associated with the accumulation of ECM proteins leads to cirrhosis with high morbidity and mortality (1). Currently antifibrotic therapies mainly focus on targeting profibrogenic cytokines and activated myofibroblasts (2), which are primarily derived from hepatic stellate cells (HSCs), the liver-specific mesenchymal cells essential for liver physiology and fibrosis (1). However, mechanisms and strategies on how to activate hepatic resident cellular sources such as hepatic progenitor cells (HPCs) to regenerate hepatocytes in the presence of fibrogenic insults *in vivo* have not been adequately investigated.

The liver has a remarkable capacity for regeneration upon injury, a process that is driven primarily by the proliferation of mature hepatocytes (3). Hepatocytes are metabolically active cells in the liver that make up 70–80% of the liver mass. The other differentiated epithelial cell type in the liver, cholangiocytes, form the biliary network. When the ability of hepatocyte proliferation is compromised, liver repopulation occurs through the activation of 'oval cells', the quiescent HPCs residing within the canals of Hering, extensions of the portal bile ductules (4). Genetic lineage tracing suggested that *Sox9, Foxl1*, and *Lgr5* expression marks these progenitor cells that give rise to both hepatocytes and cholangiocytes *in vivo* (5–7). Furthermore, by using ductal cell surface-marking antibodies, subpopulations of liver cells from normal adult mice or those undergoing an oval cell response were isolated and their capacity to form bi-lineage colonies *in vitro* was confirmed (8). Nonetheless, whether oval cells are species-specific and/or hepatic insults-specific, or conserved across these variations remains unresolved. Challenges in studying these cells *in vivo* deter full comprehension of their cellular behavior.

It has been shown that interactions between signaling pathways are critical for the fate commitment of HPCs during liver regeneration (9). In the case of biliary damage, a cell-cell interaction between Notch-expressing HPCs and Jagged1-expressing myofibroblasts acts as the default pathway to specify biliary cell fate in HPCs (9). In parallel, Wnt3a, secreted by macrophages in reaction to phagocytosis of apoptotic hepatocytes, suppresses a default Notch signaling in HPCs through an induction of Notch antagonist NUMB (10), a direct target of the canonical-Wnt signaling (11), leading HPCs to attain the hepatocyte lineage (9). Furthermore, activity of Wnt reporter *Axin-lacZ* was upregulated upon liver injury by carbon tetrachloride (CCl_4) injection. Subsequently, many Wnt target genes, including *Lgr5*, were induced in the groups of small cells near the biliary ducts, which contribute to hepatocytes and cholangiocytes during the repair phase (7). Nevertheless, the pivotal question of how the underlying signaling pathways and cell-cell communications orchestrate the distinct cellular responses of the HPCs in different contexts of hepatic insults remain elusive. In particular, the link between the signal(s) responsible for specification of HPCs towards the biliary or hepatocyte lineage and the one(s) leading to the expansion of the HPCs awaits further investigation.

The zebrafish, *Danio rerio*, has emerged as an invaluable vertebrate model system for studying regeneration, possessing a range of molecular, cellular, and genetic tools needed to thoroughly investigate underlying processes and/or mechanisms of regeneration (12). The composition, structure, function, and genetic control of the liver are relatively conserved between zebrafish and mammals (13). With transgenic strategies for expressing fluorescent

proteins in different hepatic cell types, we could visualize hepatic cell behaviors at the single-cell level along with real-time *in vivo* imaging. Furthermore, we could perform genetic and chemical screens to discover regulators of liver development, disease, and regeneration in a cost- and time-effective way (13). Recent, comprehensive studies have discovered conserved and/or novel genes and pathways that regulate liver development and pathogenesis in zebrafish (14–15). However, few studies have effectively modeled liver regeneration in response to sustained fibrogenic stimuli of chronic liver disease with zebrafish.

In this study, we established a zebrafish model to delineate the molecular and cellular mechanisms that mediate the effects of sustained fibrogenic insult on hepatocyte regeneration. We identified a subset of HPCs that experiences different levels of Notch signaling, which in turn is essential for hepatocyte regeneration. Lower levels of Notch signaling promote proliferation and subsequent differentiation of these cells into hepatocytes, while high levels of Notch signaling suppress hepatocyte regeneration. Through chemical screens, we pinpointed a number of Wnt agonists and Notch antagonists that facilitate hepatocyte regeneration. We further determined that these Wnt agonists suppress Notch signaling by inducing a Notch antagonist Numb. These data suggest an essential interplay between Wnt and Notch signaling during hepatocyte regeneration in the fibrotic liver, providing legitimate therapeutic strategies for chronic liver failure *in vivo*.

MATERIALS AND METHODS

Zebrafish lines

Animals received humane care according to the criteria of the National Institutes of Health and the Georgia Institute of Technology Institutional Animal Care and Use Committee. The generation of nitroreductase constructs to establish a hepatocyte-specific genetic ablation system and zebrafish transgenic lines are described in the supporting materials and methods.

Ethanol and Metronidazole treatment

To ablate hepatocytes, the larvae (15mM, 24–36 hours) or adult fish (10mM, 8 hours) were treated with Metronidazole (MTZ, Sigma-Aldrich, St. Louis, MO). The MTZ was then washed out, marking the 0 hours-post-ablation (hpa) point. For ethanol (EtOH) treatment, the larvae were pretreated with 1.5% EtOH (Sigma-Aldrich, St. Louis, MO) for 24 hours and then concurrently treated with MTZ for 24 hours. For the adult fish, we pretreated the fish with 1% EtOH for 72 hours and followed with MTZ treatment.

Immunohistochemistry, 5-Ethynyl-2'-Deoxyuridine (EdU) cell-cycle analysis and chemical treatment

Immunohistochemistry, EdU cell-cycle analysis, and chemical treatment were performed as previously described (16). Further details are described in the supporting materials and methods.

Quantitative real-time polymerase chain reaction, reporter assay and chemical screens

Materials and methods for these experiments are described in the supporting materials and methods.

RESULTS

Establishing a model of sustained fibrotic liver in zebrafish

To establish a clinically relevant fibrotic liver model in zebrafish, we induced near-complete eradication of hepatocytes in the presence of fibrogenic insult. First, we generated two transgenic lines, *Tg(fabp10a:CFP-NTR)*^{gt1} and *Tg(fabp10a:mCherry-NTR)*^{gt2}, to specifically ablate hepatocytes in the liver. Nitroreductase (NTR) converts the nontoxic prodrug Metronidazole (MTZ) into a DNA interstrand cross-linking agent, which induces cell death (17–19). Treatment of MTZ from 84–90 hours-post-fertilization (hpf) when the hepatocytes and biliary epithelial cells have differentiated (20), effectively ablated the hepatocytes (Supporting Fig. 1) in the presence of hepatic endothelial cells (Supporting Fig. 2E) and HSCs (Supporting Fig. 2F). We additionally utilized two transgenic lines, *Tg(Tp1:EGFP)*^{um14} and *Tg(Tp1:mCherry)*^{jh11} (21), which mark Notch signaling experiencing cells (Notch-responsive cells, NRCs) with EGFP and nuclear mCherry, respectively, under the control of the TP1 module containing multiple RBP-Jk-binding sites (Supporting Fig. 1B, F). Confocal analyses showed that the pattern of hepatic EGFP or mCherry expression significantly overlapped with the distribution of the 2F11 epitope, which marks intrahepatic biliary epithelia (22) (data not shown). At 0 hours-post-ablation (hpa), MTZ-mediated damaged livers showed substantial reduction or complete absence of hepatocytes, leading to a collapsed liver, while EGFP- or nuclear mCherry-positive NRCs remained (Supporting Fig. 1D, H, 2D).

We examined the cellular events of hepatocyte regeneration with or without 1.5% ethanol (EtOH) in [*Tg(fabp10a:CFP-NTR)*^{gt1}*; Tg(Tp1:mCherry)*^{jh11}; *Tg(hand2:EGFP)*^{pd24}] (23)] larvae. We observed an expansion of HSCs in the MTZ-treated regenerating livers without EtOH treatment (Fig. 1B', Supporting Fig. 3B'). In the presence of EtOH, as previously reported (24), HSCs increased in number (Fig. 1C', Supporting Fig. 3C') with the altered morphology from a star-like configuration to a myofibroblast-like shape with lost cytoplasmic processes (Fig. 1C', Supporting Fig. 3C', insets). Furthermore, production of ECM proteins, detected by laminin and fibrillar type I collagen (1, 2), was significantly augmented in the EtOH/MTZ-treated regenerating livers, suggesting that EtOH exposure triggers fibrogenic changes (Fig. 1C", D, Supporting Fig. 3C", D). Nevertheless, hepatocyte regeneration proceeded (Fig. 1C, C"', Supporting Fig. 3C, C"') at a lower efficiency (Fig. 1E, Supporting Fig. 3E).

Intriguingly, in the MTZ-treated regenerating livers at 50 hpa, we noticed a population of cells co-expressing hepatocyte-specific CFP and NRC-specific mCherry regardless of EtOH treatment (Fig. 1B"', C"', Supporting Fig. 3B"', C"', insets with arrows). The CFP and dim mCherry co-expressing NRCs are distinguishable from the bright red NRCs that are negative for CFP and positive for Activated leukocyte cell adhesion molecule (Alcam), a biliary epithelial cell marker (20) (Supporting Fig. 4B", C", insets with arrowheads). The co-

expressing cells were not detected in the EtOH only-treated larvae (Supporting Fig. 4D"', inset). Similar to that observed in the larvae, the CFP and dim mCherry co-expressing cells were detected both in the MTZ- and EtOH/MTZ-treated regenerating livers of 12-month-old [*Tg(fabp10a:CFP-NTR)*^{gt1}*; Tg(Tp1:mCherry)*^{jh11}] adult fish at 3 days-post-ablation (dpa) (Fig. 2E", F", insets with arrows) with markedly elevated deposition of type I collagen in the presence of EtOH (Fig. 2F', G, H). Given the facts that the quiescent HPCs reside in the bile ductules (4) and the proliferation of HSCs and the expansion of HPCs occur concurrently in the partial hepatectomy model with compromised hepatocyte proliferation in mammals (25), these data indicate that the CFP and dim mCherry co-expressing NRCs represent a zebrafish-counterpart of HPCs that differentiate into hepatocytes by experiencing lower levels of Notch signaling. Furthermore, these results suggest that even in the presence of sustained fibrogenic insult such as EtOH, the HPCs, responsive to Notch signaling, maintain their capacity to regenerate as hepatocytes.

Heterogeneity of Notch signaling activity in the regenerating livers

We further investigated the relationship between heterogeneity of Notch signaling and hepatocyte regeneration by performing time-course analyses in [*Tg(fabp10a:CFP-NTR)*^{gt1}*; Tg(Tp1:mCherry)*^{jh11}] larvae. Compared with the DMSO-treated controls, MTZ treatment led to the destruction of layers of hepatocytes, resulting in NRCs in closer proximity to each other (Fig. 3A). The number of mCherry-expressing NRCs increased at 5 hpa with two discrete populations of dimming red NRCs (Fig. 3B, inset with arrows) and bright red NRCs (Fig. 3B, inset with arrowheads). At 13–15 hpa, hepatocyte-specific CFP began to appear and co-expressed in a few dimming mCherry-positive NRCs throughout the regenerating livers (Fig. 3C, inset with arrows). The remaining bright red NRCs (Fig. 3C, inset with arrowhead) suggested a NRC-to-hepatocyte conversion in a subset of NRCs. These CFP and mCherry co-expressing NRCs continued to increase in number, resulting in two clearly distinct heterogeneous populations of NRCs: dim red NRCs co-expressing CFP (Fig. 3D', D", insets with arrows) and the bright red NRCs without CFP markers (Fig. 3D', D", insets with arrowheads). The former gradually became CFP only-positive cells with the loss of red, suggesting that they differentiated into hepatocytes and may no longer be subject to Notch signaling (Fig. 3E', E", insets with arrows). The percentage of dim red NRCs increased during regeneration with all of the CFP-positive hepatocytes being derived from these cells (Fig. 3G). By 70 hpa, the conversion was nearly complete (Fig. 3F), resulting in the repopulation of the entire liver with newly generated functional hepatocytes, which processed PED6, a fluorescent fatty acid reporter (26) at 96 hpa (Supporting Fig. 5 C, arrow). The larvae continued to express Alcam and restored the expression of Abcb11, a bile transport pump (27) located in the bile canaliculi of hepatocytes at 96 hpa (Supporting Fig. 5F, J) and 1-months-post-ablation (mpa) (Supporting Fig. 5G, K). This indicated that the liver function was recovered and maintained after near-complete eradication of hepatocytes. Similar regeneration events occurred in the EtOH/MTZ-treated regenerating livers but at a slower efficiency (Supporting Fig. 6) and a decreased recovery of liver function (Supporting Fig. 5 D, H, L). Furthermore, regardless of EtOH treatment, we detected comparable occurrences in [*Tg(fabp10a:mCherry-NTR)*^{gt2}*; Tg(Tp1:EGFP)*^{um14}] larvae (Supporting Fig. 7, insets), while other differentiated liver cells including endothelial cells and HSCs had minimum capacity to convert into hepatocytes (Supporting Fig. 8B, D, insets). These data

indicate that NRCs experience different levels of Notch signaling during hepatocyte regeneration; the HPCs with continuously lower levels of Notch activity differentiate into hepatocytes, while those with higher levels remain as cholangiocytes.

To further examine the contribution of the HPCs to regenerating hepatocytes, we used the [*Tg(Tp1:CreERT2)*^{jh12}; *Tg(actb2:loxP-STOP-loxP-hmgb1-mCherry)*^{jh15}] (28) lines, in which nuclear mCherry expression is genetically induced in NRCs. Treating tamoxifen either prior to (24–48 hpf) or after (0–24 hpa) hepatocyte ablation, we detected a subset of mCherry-expressing NRCs which co-expressed hepatocyte-specific CFP at 35 hpa (Supporting Fig. 9 B, B', D, D', arrows) and 1 mpa (Supporting Fig. 9E, F, arrows). In the control livers without MTZ treatment, mCherry-expressing NRCs were only detected in the Alcam-positive biliary epithelial cells but not in the hepatocytes (Supporting Fig. 9A, C, yellow arrowheads). Altogether, these data suggest that NRCs portray two populations of cells: the cholangiocytes and the HPCs, which represent a progenitor population with the potential to regenerate as hepatocytes.

Distinct levels of Notch signaling are essential for the proliferation and differentiation of the HPCs

To analyze how the discrete levels of Notch signaling regulate the fate of HPCs, we first examined the dynamics of Notch signaling in the MTZ-treated regenerating livers. We utilized transgenic lines expressing a destabilized fluorescent protein with a short half-life (VenusPEST) and a fluorescent protein with enhanced stability (Histone2BmCherry) under the Notch responsive TP1 element, *Tg(Tp1:VenusPEST)*^{s939} and *Tg(Tp1:H2BmCherry)*^{s940}, respectively (16). Thus, the *Tg(Tp1:*H2BmCherry); *Tg(Tp1:*VenusPEST)-double positive cells are presently experiencing Notch signaling, whereas the *Tg(Tp1:*H2BmCherry)-positive; *Tg(Tp1:*VenusPEST)-negative cells were positive for Notch signaling in their recent past but have since switched it off. In the control livers, there was a clear overlap between *Tg(Tp1:*H2BmCherry) and *Tg(Tp1:*VenusPEST) expression with a small number of *Tg(Tp1:*H2BmCherry)-single positive NRCs (Fig. 4A, white arrowheads). Alcam is expressed in all of the *Tg(Tp1:*H2BmCherry)-positive NRCs. At 0 hpa in the MTZ-treated livers, we observed the heterogeneity in the expression of Venus, segregating *Tg(Tp1:*H2BmCherry)-positive NRCs into 3 groups based on Venus intensity and Alcam expression: *Tg(Tp1:*VenusPEST)^{high}/Alcam^{+}, *Tg(Tp1:*VenusPEST)$^{-}$/Alcam^{-}, and *Tg(Tp1:*VenusPEST)^{low}/Alcam^{+} cells (Fig. 4B, yellow arrowheads, white arrowhead, and red arrowheads, respectively). At 5–10 hpa, the proportion of *Tg(Tp1:*VenusPEST)$^{-}$/Alcam^{-} cells (Fig. 4C–D', G, white arrowheads) started increasing in the regenerating livers with a decrease in *Tg(Tp1:*VenusPEST)^{low}/Alcam^{+} cells (Fig. 4C–D', G, red arrowheads), implying that the latter had begun to turn off Notch signaling and initiated the differentiation into hepatocytes. At 13–15hpa, when a NRC-to-hepatocyte conversion occurs, all the converting CFP-positive NRCs were *Tg(Tp1:*VenusPEST)$^{-}$/Alcam^{-} cells (Fig. 4E, G, white arrows). Consistently, at 25 hpa, there was a near absence of *Tg(Tp1:*VenusPEST)^{low}/Alcam^{+} cells with virtually all the CFP-positive cells being *Tg(Tp1:*VenusPEST)$^{-}$/Alcam^{-} cells (Fig. 4F, G, white arrows), while *Tg(Tp1:*VenusPEST)^{high}/Alcam^{+} cells did not express CFP (Fig. 4F, yellow arrowheads). These data suggest that *Tg(Tp1:*VenusPEST)^{high}/Alcam^{+} cells may correspond to the cholangiocytes, whereas

*Tg(Tp1:*VenusPEST)^{low}/Alcam^{+} and *Tg(Tp1:*VenusPEST)$^{-}$/Alcam^{-} cells experiencing different degrees of Notch downregulation at early stages of liver regeneration likely equate to the transitioning HPCs, giving rise to newly generated hepatocytes (*Tg(Tp1:*VenusPEST)$^{-}$/Alcam^{-}/CFP^{+} cells). Comparable dynamics of Notch signaling were detected in the EtOH/MTZ-treated regenerating livers at a slower efficiency of regeneration (Supporting Fig. 10). Further analysis of Notch activity by comparing the expression dynamics of VenusPEST and mCherry, of which the half-life is comparable to that of GFP (29), revealed two distinct populations of mCherry-positive cells at 0 hpa: bright and dim red (Supporting Fig. 11A, A', G). The latter was only present in the *Tg(Tp1:*VenusPEST)$^{-}$/Alcam^{-} group with a significant increase in percentage between 15 and 25 hpa (Supporting Fig. 11G), suggesting a small population of cells that is more responsive to Notch signaling even 'during' ablation.

We further determined the correlation between the levels of Notch signaling and proliferation by performing cell cycle analysis with the replication marker 5-ethynyl-2'-deoxyuridine (EdU). In the MTZ-treated regenerating livers between 0–10 hpa (before hepatocyte-specific CFP began to appear), we detected a more pronounced increase of EdU incorporation in the NRCs with lower levels of *Tg(Tp1:*VenusPEST) expression than in those with higher levels of expression (Fig. 5A–B). While hyper-activating Notch signaling suppressed differentiation into hepatocytes (Supporting Fig. 12G–I), strong downregulation of Notch signaling increased differentiation regardless of EtOH treatment (Supporting Fig. 12A–F). Altogether, these data suggest that the HPCs encounter discrete levels of Notch downregulation, which is essential for triggering a multi-step process of proliferation and subsequent differentiation of these cells into regenerating hepatocytes.

Chemical screens reveal the critical role of Wnt signaling in hepatocyte regeneration in the presence of sustained fibrogenic stimulus

To identify bioactive compounds that facilitate hepatocyte regeneration in the fibrotic liver, we performed chemical genetic screens. We screened a library of 75 small molecules with well-characterized biological and pharmaceutical activity using [*Tg(fabp10a:CFP-NTR)*^{gt1}; *Tg(Tp1:VenusPEST)*^{s940}] larvae in the presence or in the absence of 1.5% EtOH. Several γ-secretase inhibitors known to block Notch signaling such as Semagacestat and YO-01027, enhanced hepatocyte regeneration (Supporting Table 1). Interestingly, a number of Wnt agonists such as SB 415286 and CHIR-99021, inhibitors of glycogen synthase kinase-3, promoted hepatocyte regeneration (Fig. 6A–C, Supporting Table 1). In contrast, a Wnt antagonist, XAV-939, inhibited regeneration (Supporting Table 1). We further screened 1,000 small molecules from 0 to 50 hpa in hepatocyte-ablated larvae. Sixteen compounds showed various degrees of activity of accelerating hepatocyte regeneration. Two of the compounds, [bisbenzyldimethylamine, chloride] and [4-(1H-1,2,3,4-tetraazol-5-yl)-1,2,5-oxadiazole-3-ylamine], showed significantly enhanced activity in the Topflash reporter, which is responsive to β-catenin-mediated canonical Wnt signaling (Fig. 6G), suggesting that the identified compounds are novel canonical Wnt pathway activators with the capacity to enhance hepatocyte regeneration (Fig. 6H, I). Importantly, the Wnt agonists that were tested augmented hepatocyte regeneration in the EtOH/MTZ-treated livers (Fig. 6D–F, J, K). These data suggest that the canonical Wnt signaling plays an essential role in hepatocyte

regeneration even in the presence of sustained fibrogenic insult. Furthermore, the screening approach provides an invaluable tool to identify small molecules that accelerate hepatocyte regeneration.

Wnt signaling antagonizes Notch signaling to promote hepatocyte regeneration in the presence of sustained fibrogenic stimulus

During the chemical screens, we observed that Wnt agonists accelerating hepatocyte regeneration induced downregulation of *Tg(Tp1:*VenusPEST) expression without a detrimental effect on biliary secretion (Fig. 7A, B, Supporting Fig. 13A, C, E). Hence, we hypothesized that the antagonistic interaction of Wnt and Notch signaling plays an essential role in regulating the regenerative capacity of HPCs. To test this hypothesis, we examined the expression of *numb*, a direct transcriptional target of Wnt signaling that functions as a Notch antagonist (9–11), and found that its mRNA level was significantly upregulated in the MTZ-treated regenerating livers (Fig. 7G). Wnt agonist identified from the chemical screens augmented the levels of *numb* expression both in the MTZ- (Fig. 7H) and EtOH/MTZ- (Fig. 7I) treated regenerating livers, suggesting that the attenuation of Notch signaling is closely associated with the activation of Wnt signaling. Furthermore, Wnt agonist significantly increased the total percentage of CFP-positive hepatocytes and *Tg(Tp1:*VenusPEST)$^{-}$/Alcam^{-} cells, in which all CFP-positive hepatocytes were derived from, regardless of EtOH treatment (Fig. 7C, F), while decreasing that of *Tg(Tp1:*VenusPEST)^{low}/Alcam^{+} cells (Fig. 7C, F). These data imply that the Wnt agonist treatment results in sustained inhibition of Notch activity in the HPCs and enhanced differentiation of these cells into hepatocytes. Genetic induction of Wnt signaling significantly accelerated regeneration (Supporting Fig. 14A–C), while its inhibition suppressed the efficiency of regeneration (Supporting Fig. 14D–F). Altogether, our study suggests that the Wnt-Notch interplay mediated by Numb is pivotal to hepatocyte regeneration even in the presence of sustained fibrogenic stimulus, providing fundamental clues for designing therapeutic targets for chronic liver failure *in vivo*.

DISCUSSION

Here we present a zebrafish model to elucidate the molecular and cellular mechanisms of hepatocyte regeneration in the presence of sustained fibrogenic insult. We induced near-complete eradication of hepatocytes and used EtOH as a fibrogenic stimulus. In this model, we identified a subset of HPCs, responsive to Notch signaling, that maintains its capacity to regenerate as hepatocytes (Fig. 8). This finding implies that modulating the proliferation and differentiation of these Notch responsive HPCs in the fibrotic liver may increase hepatocyte regeneration. We pinpointed a number of Wnt agonists and Notch antagonists facilitating hepatocyte regeneration through chemical screens. Further analyses demonstrated that these Wnt agonists attenuate Notch signaling by inducing a Notch antagonist, Numb, suggesting that the Wnt-Notch interplay crucially affects hepatocyte regeneration in the fibrotic liver. Manipulating this antagonistic interplay may stimulate hepatocyte regeneration, presenting viable therapeutic strategies for chronic liver failure *in vivo*.

Activation of Wnt3a/β-catenin signaling through the induction of NUMB was shown to attenuate a default Notch signaling, promoting HPCs to differentiate into hepatocytes in the Choline Deficient-Ethionine supplemented diet (9). Our analyses identify the mechanisms of how the opposing interaction between Wnt and Notch signaling directs the specific and distinct cellular outcomes of the HPCs in the presence of EtOH as a fibrogenic stimulus, suggesting that the mechanism of HPC activation may be conserved across species and different categories of hepatic insults. Our data further suggest that the HPCs may have different responsiveness to the Wnt-Notch interplay. *Tg(Tp1:*mCherry*)*^{dim}/*Tg(Tp1:*VenusPEST$)^{-}$/Alcam^{-} cells at 0 hpa may correspond to the HPCs that are responsive to initial Wnt activity. As hepatocyte ablation proceeds, the HPCs are in closer proximity, encountering concentrated Wnt signaling and progressing from *Tg(Tp1:*VenusPEST$)^{low}$/Alcam^{+} to *Tg(Tp1:*VenusPEST$)^{-}$/Alcam^{-} cells with concurrent downregulation of Notch activity and proliferation to give rise to *Tg(Tp1:*VenusPEST$)^{-}$/Alcam^{-}/CFP^{+} hepatocytes. Whether the HPCs have divergent Wnt-Notch reactivity and differentiation potencies depending on their location awaits further study. While the putative HPCs are often thought to reside within the canals of Hering, which are located at the terminal branches of the biliary tree, multiple lines of work suggest that HPCs may exist throughout the biliary network and even in the common bile duct (30). Given that there is a number of cells with low expression of VenusPEST in non-ablated wild-type livers (Fig. 4A), it is plausible to speculate that these cells correspond to a subpopulation of the HPCs in zebrafish, which equate to the *Tg(Tp1:*mCherry*)*^{dim}*/Tg(Tp1:*VenusPEST$)^{-}$/Alcam^{-} cells; these cells are more responsive to the initial difference of Wnt gradient in setting up a primary bias in Notch activity (9). In this regard, it is intriguing that the NRCs in the proximal region, which form large ducts contiguous with the extrahepatic duct and portal vein, have a tendency to lose Notch signaling more quickly and are more responsive to Notch inhibition than distal cells (31). However, it is likely that the majority of the HPCs distribute throughout the hepatic parenchyma. *in vivo* and three-dimensional analyses in medaka (*Oryzias latipes*) suggest that the bile preductular epithelial cells (BPDECs), the putative counterpart of mammalian hepatic progenitors, are localized to the intrahepatic biliary passageways (IHBP), which occupy 95% of the liver corpus uniformly (32). Similarly, bile preductules situated between the canaliculi and bile ductules in zebrafish may correspond to the canals of Hering in mammals (33). BPDECs constitute the majority of biliary epithelial cells in the zebrafish liver and directly contact hepatocytes with no basal lamina (33). A multicolor clonal analysis using an adapted version of the Brainbow Cre-*lox* mediated recombination system (34) will allow us to trace and distinguish the location and the fates of individual HPCs that contribute to regenerating hepatocytes in the presence of divergent hepatic insults.

As NRCs encompass not only HPCs but also cholangiocytes, it will be worth considering the possibility of contribution of these differentiated cells to regenerating hepatocytes in the presence of fibrogenic insults. Recent studies have shown that after near total loss of hepatocytes in zebrafish, hepatic biliary epithelial cells transdifferentiated into hepatocytes through a step of dedifferentiation with the assumption that cholangiocytes solely constitute NRCs (35, 36). While we are not able to exclude the possibility of the transdifferentiation in hepatocyte regeneration, our studies indicate that the HPCs, which are more susceptible to

Wnt-Notch interplay, encounter discrete levels of Notch downregulation at early stages of hepatocyte regeneration with subsequent differentiation into hepatocytes, while cholangiocytes maintain higher levels of Notch activity. Identification and combination of bona fide cholangiocyte and active HPC markers with genetic fate mapping strategies will enable us to further dissect the behavior of these cells at the molecular and cellular levels.

Inducing tissue regeneration via stem or progenitor cells while delaying fibrosis has been on the rise as antifibrogenic strategies of great potential. Our studies investigating the effects of sustained fibrogenic stimulus in hepatocyte regeneration using zebrafish will give us a clue towards how to direct the differentiation of autologous hepatic progenitor cells into hepatocytes in human patients harboring mature fibrotic scar tissue derived from chronic liver failure. Our work further demonstrates that the fibrotic liver model in zebrafish represents a superb chemical screening system with noteworthy advantages over cell culture- or mammalian-based screening system. It is an *in vivo* system with significant cost- and time-saving benefits. Moreover, given the fact that the composition, structure, function, and genetic control of the liver are relatively conserved between zebrafish and mammals (13), small molecules effective in zebrafish are highly likely to be active and applicable in the mammalian system. Overall, employing the *in vivo*-based hepatic regeneration strategy may allow us to overcome fundamental drawbacks in stem cell therapy, opening up new avenues of endogenous cellular regeneration therapy.

Supplementary Material

Refer to Web version on PubMed Central for supplementary material.

Acknowledgments

The authors thank Drs. Ryan Anderson, Neil Chi, Suk-Won Jin, Young-Sup Yoon, and Chris Yun for their critical comments and support, Dr. Michael Parsons for transgenic fish lines, Dr. Francesca Storici for the cell culture facility, Dr. Manu Platt for the HEK293T cell line, and Jin Xu for technical assistance. The authors acknowledge the Biomolecular Analysis core and the Microscopy and Biophotonics core at the Parker H. Petit Institute for Bioengineering and Bioscience at Georgia Tech for technical support.

Financial support:

Chong Hyun Shin is supported by Grant number K01DK081351 from the National Institutes of Health (NIH), the Regenerative Engineering and Medicine Research Center Pilot Award (GTEC 2731336), and a start-up package from the School of Biology, Georgia Institute of Technology.

Abbreviations

ECM	extracellular matrix
HPC	hepatic progenitor cell
HSC	hepatic stellate cell
CCl_4	carbon tetrachloride
EtOH	ethanol
MTZ	Metronidazole

DMSO	dimethyl sulfoxide
4-OHT	4-Hydroxytamoxifen
EdU	5-ethynyl-2'-deoxyuridine
fabp10	fatty acid binding protein 10
CFP	cyan fluorescent protein
NTR	nitroreductase
hpf	hours-post-fertilization
EGFP	enhanced green fluorescent protein
NRC	Notch-responsive cell
hpa	hours-post-ablation
dpf	days-post-fertilization
Alcam	activated leukocyte cell adhesion molecule
DAPT	N-[N-(3,5-Difluorophenacetyl)-L-alanyl]-S-phenylglycine t-butyl ester
qPCR	quantitative polymerase chain reaction
BPDEC	bile preductular epithelial cell
IHBP	intrahepatic biliary passageway

REFERENCES

1. Hernandez-Gea V, Friedman SL. Pathogenesis of liver fibrosis. Annu Rev Pathol. 2011; 6:425–456. [PubMed: 21073339]
2. Kisseleva T, Brenner DA. Anti-fibrogenic strategies and the regression of fibrosis. Best Pract Res Clin Gastroenterol. 2011; 25:305–317. [PubMed: 21497747]
3. Michalopoulos GK. Liver regeneration. J Cell Physiol. 2007; 213:286–300. [PubMed: 17559071]
4. Turner R, Lozoya O, Wang Y, Cardinale V, Gaudio E, Alpini G, et al. Human hepatic stem cell and maturational liver lineage biology. Hepatology. 2011; 53:1035–1045. [PubMed: 21374667]
5. Furuyama K, Kawaguchi Y, Akiyama H, Horiguchi M, Kodama S, Kuhara T, et al. Continuous cell supply from a Sox9-expressing progenitor zone in adult liver, exocrine pancreas and intestine. Nat Genet. 2011; 43:34–41. [PubMed: 21113154]
6. Shin S, Walton G, Aoki R, Brondell K, Schug J, Fox A, et al. Foxl1-Cre-marked adult hepatic progenitors have clonogenic and bilineage differentiation potential. Genes Dev. 2011; 25:1185–1192. [PubMed: 21632825]
7. Huch M, Dorrell C, Boj SF, van Es JH, Li VS, van de Wetering M, et al. In vitro expansion of single Lgr5+ liver stem cells induced by Wnt-driven regeneration. Nature. 2013; 494:247–250. [PubMed: 23354049]
8. Dorrell C, Erker L, Schug J, Kopp JL, Canaday PS, Fox AJ, et al. Prospective isolation of a bipotential clonogenic liver progenitor cell in adult mice. Genes Dev. 2011; 25:1193–1203. [PubMed: 21632826]
9. Boulter L, Govaere O, Bird TG, Radulescu S, Ramachandran P, Pellicoro A, et al. Macrophage-derived Wnt opposes Notch signaling to specify hepatic progenitor cell fate in chronic liver disease. Nat Med. 2012; 18:572–579. [PubMed: 22388089]
10. Guo M, Jan LY, Jan YN. Control of daughter fates during asymmetric division: interaction of Numb and Notch. Neuron. 1996; 17:27–41. [PubMed: 8755476]

11. Katoh M, Katoh M. NUMB is a break of WNT-Notch signaling cycle. Int J Mol Med. 2006; 18:517–521. [PubMed: 16865239]
12. Poss KD. Advances in understanding tissue regenerative capacity and mechanisms in animals. Nat Rev Genet. 2010; 11:710–722. [PubMed: 20838411]
13. Chu J, Sadler KC. New school in liver development: lessons from zebrafish. Hepatology. 2009; 50:1656–1663. [PubMed: 19693947]
14. Field HA, Ober EA, Roeser T, Stainier DY. Formation of the digestive system in zebrafish. I. Liver morphogenesis. Dev Biol. 2003; 253:279–90. [PubMed: 12645931]
15. Ober EA, Verkade H, Field HA, Stainier DY. Mesodermal Wnt2b signaling positively regulates liver specification. Nature. 2006; 442:688–91. [PubMed: 16799568]
16. Ninov N, Borius M, Stainier DY. Different levels of Notch signaling regulate quiescence, renewal and differentiation in pancreatic endocrine progenitors. Development. 2012; 139:1557–1567. [PubMed: 22492351]
17. Curado S, Anderson RM, Jungblut B, Mumm J, Schroeter E, Stainier DY. Conditional targeted cell ablation in zebrafish: a new tool for regeneration studies. Dev Dyn. 2007; 236:1025–1035. [PubMed: 17326133]
18. Pisharath H, Rhee JM, Swanson MA, Leach SD, Parsons MJ. Targeted ablation of beta cells in the embryonic zebrafish pancreas using E. coli nitroreductase. Mech Dev. 2007; 124:218–29. [PubMed: 17223324]
19. Curado S, Stainier DYR, Anderson RM. Nitroreductase-mediated cell/tissue ablation in zebrafish: a spatially and temporally controlled ablation method with applications in developmental and regeneration studies. Nature Protoc. 2008; 3:948–954. [PubMed: 18536643]
20. Sakaguchi TF, Sadler KC, Crosnier C, Stainier DY. Endothelial signals modulate hepatocyte apicobasal polarization in zebrafish. Curr Biol. 2008; 18:1565–1571. [PubMed: 18951027]
21. Parsons MJ, Pisharath H, Yusuff S, Moore JC, Siekmann AF, Lawson N, et al. Notch-responsive cells initiate the secondary transition in larval zebrafish pancreas. Mech Dev. 2009; 126:898–912. [PubMed: 19595765]
22. Lorent K, Moore JC, Siekmann AF, Lawson N, Pack M. Reiterative use of the notch signal during zebrafish intrahepatic biliary development. Dev Dyn. 2010; 239:855–864. [PubMed: 20108354]
23. Yin C, Kikuchi K, Hochgreb T, Poss KD, Stainier DY. Hand2 regulates extracellular matrix remodeling essential for gut-looping morphogenesis in zebrafish. Dev Cell. 2010; 18:973–984. [PubMed: 20627079]
24. Yin C, Evason KJ, Maher JJ, Stainier DY. The basic helix-loop-helix transcription factor, heart and neural crest derivatives expressed transcript 2, marks hepatic stellate cells in zebrafish: analysis of stellate cell entry into the developing liver. Hepatology. 2012; 56:1958–1970. [PubMed: 22488653]
25. Paku S, Schnur J, Nagy P, Thorgeirsson SS. Origin and structural evolution of the early proliferating oval cells in rat liver. Am J Pathol. 2001; 158:1313–1323. [PubMed: 11290549]
26. Farber SA, Pack M, Ho SY, Johnson ID, Wagner DS, Dosch R, et al. Genetic analysis of digestive physiology using fluorescent phospholipid reporters. Science. 2001; 292:1385–1388. [PubMed: 11359013]
27. Gerloff T, Stieger B, Hagenbuch B, Madon J, Landmann L, Roth J, et al. The sister of P-glycoprotein represents the canalicular bile salt export pump of mammalian liver. J Biol Chem. 1998; 273:10046–10050. [PubMed: 9545351]
28. Wang Y, Rovira M, Yusuff S, Parsons MJ. Genetic inducible fate mapping in larval zebrafish reveals origins of adult insulin-producing beta-cells. Development. 2011; 138:609–617. [PubMed: 21208992]
29. May P, Fu Y, Butler DL, Chokalingam K, Liu Y, Floret J, et al. Generation and characterization of Col10a1-mcherry reporter mice. Genesis. 2011; 49:410–418. [PubMed: 21328521]
30. Carpino G, Cardinale V, Onori P, Franchitto A, Berloco PB, Rossi M, et al. Biliary tree stem/progenitor cells in glands of extrahepatic and intraheptic bile ducts: an anatomical in situ study yielding evidence of maturational lineages. J Anat. 2012; 220:186–199. [PubMed: 22136171]

31. Delous M, Yin C, Shin D, Ninov N, Debrito Carten J, Pan L, et al. Sox9b is a key regulator of pancreaticobiliary ductal system development. PLoS Genet. 2012; 8:e1002754. [PubMed: 22719264]

32. Hardman RC, Volz DC, Kullman SW, Hinton DE. An in vivo look at vertebrate liver architecture: three-dimensional reconstructions from medaka (Oryzias latipes). Anat Rec (Hoboken). 2007; 290:770–782. [PubMed: 17516461]

33. Yao Y, Lin J, Yang P, Chen Q, Chu X, Gao C, et al. Fine structure, enzyme histochemistry, and immunohistochemistry of liver in zebrafish. Anat Rec (Hoboken). 2012; 295:567–576. [PubMed: 22271515]

34. Gupta V, Poss KD. Clonally dominant cardiomyocytes direct heart morphogenesis. Nature. 2012; 484:479–484. [PubMed: 22538609]

35. Choi T-Y, Ninov N, Stainier DY, Shin D. Extensive conversion of hepatic biliary epithelial cells to hepatocytes after near total loss of hepatocytes in zebrafish. Gastroenterology. 2014; 146:776–788. [PubMed: 24148620]

36. He J, Lu H, Zou Q, Luo L. Regeneration of liver after extreme hepatocyte loss occurs mainly via biliary transdifferentiation in zebrafish. Gastroenterology. 2014; 146:789–800. [PubMed: 24315993]

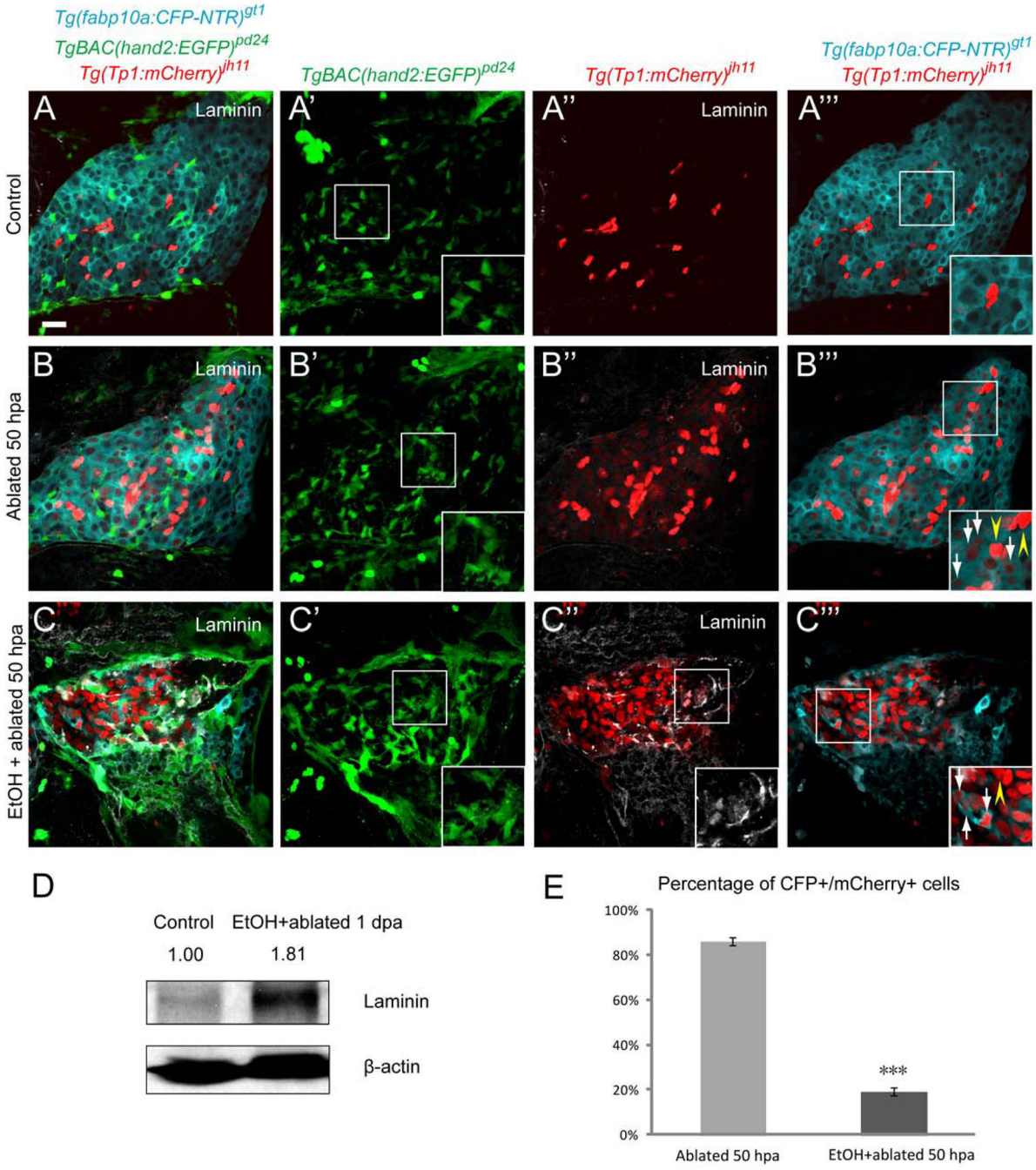

Fig. 1.

Establishing a model of sustained fibrotic liver in zebrafish. (A–A"') In [*Tg(fabp10a:CFP-NTR)*^{gt1}*; Tg(Tp1:mCherry)*^{jh11}; *Tg(hand2:EGFP)*^{pd24}] larvae treated with DMSO at 5 days-post-fertilization (dpf), quiescent HSCs showed a star-like configuration (A', inset), whereas ECM protein laminin was almost undetectable (A") and NRCs distributed among hepatocytes (A, A"'). (B–B"') Hepatocytes were ablated by MTZ and allowed to regenerate for 50 hours. In the MTZ-treated regenerating livers, the number of HSCs increased (B') with a rare deposition of laminin (B"). A population of cells co-expressing hepatocyte-

specific CFP and NRC-specific nuclear mCherry was observed throughout the MTZ-treated regenerating livers (B"', inset, white arrows) while bright red NRCs remained CFP negative (B"', inset, yellow arrowheads). (C–C"') The larvae were pretreated with 1.5% EtOH from 2.5 to 3.5 dpf and then concurrently treated with MTZ from 3.5 to 4.5 dpf and allowed to regenerate for 50 hours. HSCs increased in number and lost complex cytoplasmic processes (C', inset). Elevated laminin deposition was observed in the EtOH/MTZ-treated regenerating livers (C", inset). A population of cells co-expressing hepatocyte-specific CFP and NRC-specific nuclear mCherry was appreciated (C"', inset, white arrows) while bright red NRCs remained CFP negative (C"', inset, yellow arrowhead). (D) Representative western blot showed upregulation of laminin protein in the EtOH/MTZ-treated regenerating livers. Numbers show relative expression of laminin protein after normalization against β-actin protein. n=300 dissected larval livers per condition in three experiments. (E) Percentage (mean±SD) of CFP^+ cells in the population of *Tg(Tp1:* mCherry)-positive cells. 85.5±1.6% of *Tg(Tp1:*mCherry)-positive cells were CFP^+ in the MTZ-treated regenerating livers, while 18.7±1.8% of *Tg(Tp1:*mCherry)-positive cells expressed CFP in the EtOH/MTZ-treated regenerating livers. Cells in 5 planes of confocal images from 5 individual larvae were counted. Asterisks indicate statistical significance: ***$p<0.001$. All confocal images are single-plane images except A', B' and C', which are projection images (n=30 larvae per condition in three experiments). Scale bar, 20μm. EtOH, ethanol; SD, standard deviation.

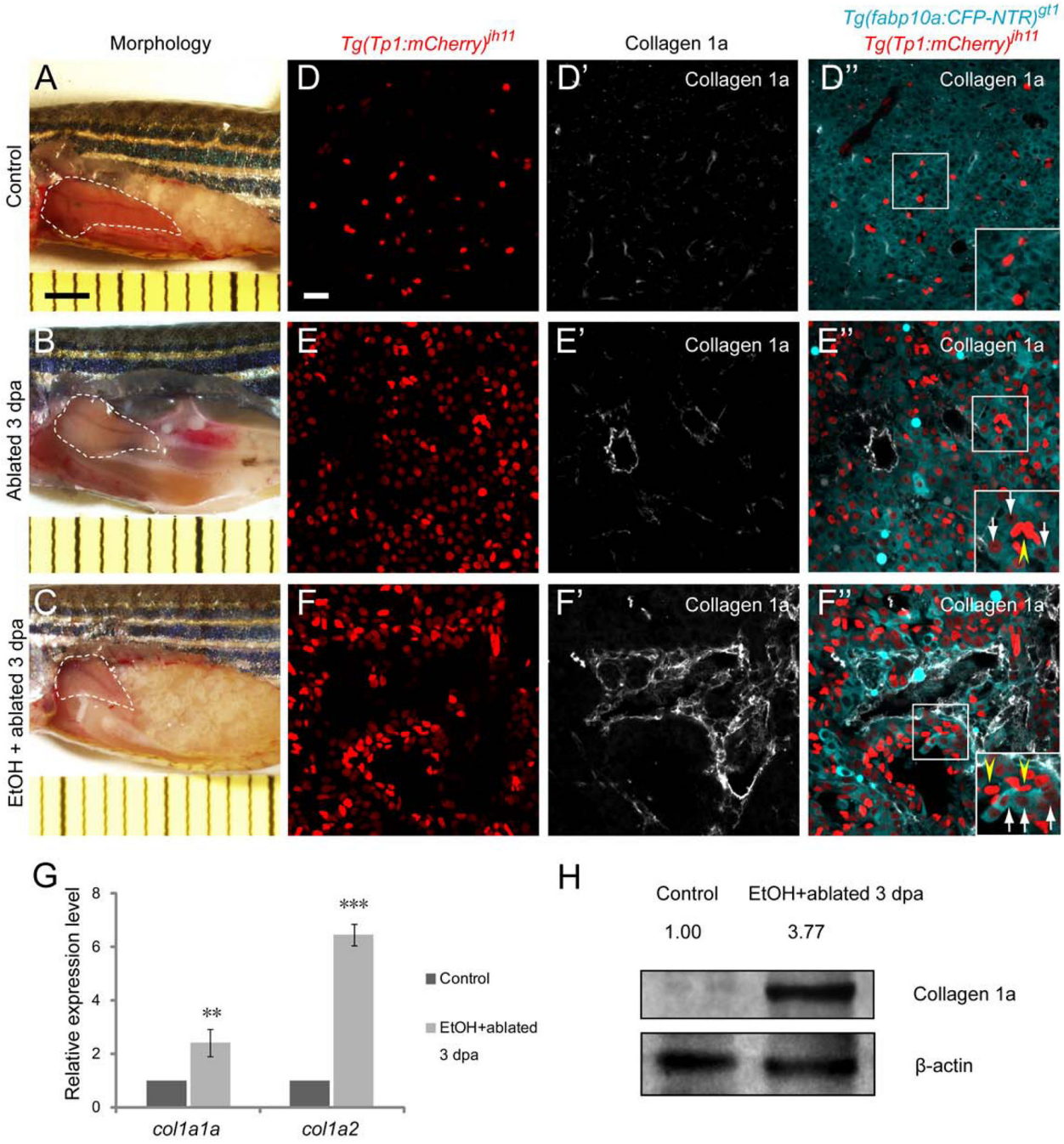

Fig. 2.

A population of cells, responsive to Notch signaling, maintains their capacity to regenerate as hepatocytes in adult zebrafish. Liver morphology (white dashed lines) of 12-month-old [*Tg(fabp10a:CFP-NTR)*^{gt1}*; Tg(Tp1:mCherry)*^{jh11}] adults treated with dimethyl sulfoxide (DMSO) (A), MTZ (B) or 1% EtOH followed by MTZ (C). (D–F") Confocal images of *Tg(fabp10a:*CFP-NTR), *Tg(Tp1:*mCherry), and type I collagen expression in vibratome sections of adult zebrafish livers. (D–D") In the DMSO-treated controls, expression of *Tg(fabp10a:*CFP-NTR) did not overlap with that of *Tg(Tp1:*mCherry) (D", inset) with

almost undetectable type I collagen deposition (D'). (E–E") Hepatocytes were ablated by 10mM MTZ treatment for 8 hours and allowed to regenerate for 3 days. Numerous cells co-expressing hepatocyte-specific CFP and NRC-specific nuclear mCherry were observed throughout the MTZ-treated regenerating livers (E", inset, white arrows) with a modest increase in type I collagen deposition (E'), while bright red NRCs remained CFP negative (E", inset, yellow arrowhead). (F–F") The fish were pretreated with 1% EtOH for 72 hours followed by 10mM MTZ treatment for 8 hours and allowed to regenerate for 3 days. Significantly elevated type I collagen deposition was observed in the EtOH/MTZ-treated regenerating livers (F'), while a population of cells co-expressing hepatocyte-specific CFP and NRC-specific nuclear mCherry was appreciated (F", inset, white arrows). The bright red NRCs remained CFP negative (F", inset, yellow arrowheads). (G) qRT-PCR analysis showed upregulation of *collagen 1a1a* and *collagen 1a2* mRNA in the EtOH/MTZ-treated regenerating livers. n=3 dissected adult fish liver per condition in three experiments. Asterisks indicate statistical significance: $^{**}p<0.01$ and $^{***}p<0.001$. (H) Representative western blot showed upregulation of type I collagen protein in the EtOH/MTZ-treated regenerating livers. Numbers show relative expression of type I collagen protein after normalization against β-actin protein. n=3 dissected adult fish liver per condition in three experiments. A–C, bright-field images. D–D", E–E", and F–F", confocal single-plane images. For each experiment, after capturing each bright-field image, the liver from the same fish was dissected and processed for section immunostaining to get confocal images (n=6 fish per condition in three experiments). Scale bars: A–C, 2mm; D–D", E–E", and F–F", 20μm. EtOH, ethanol; SD, standard deviation.

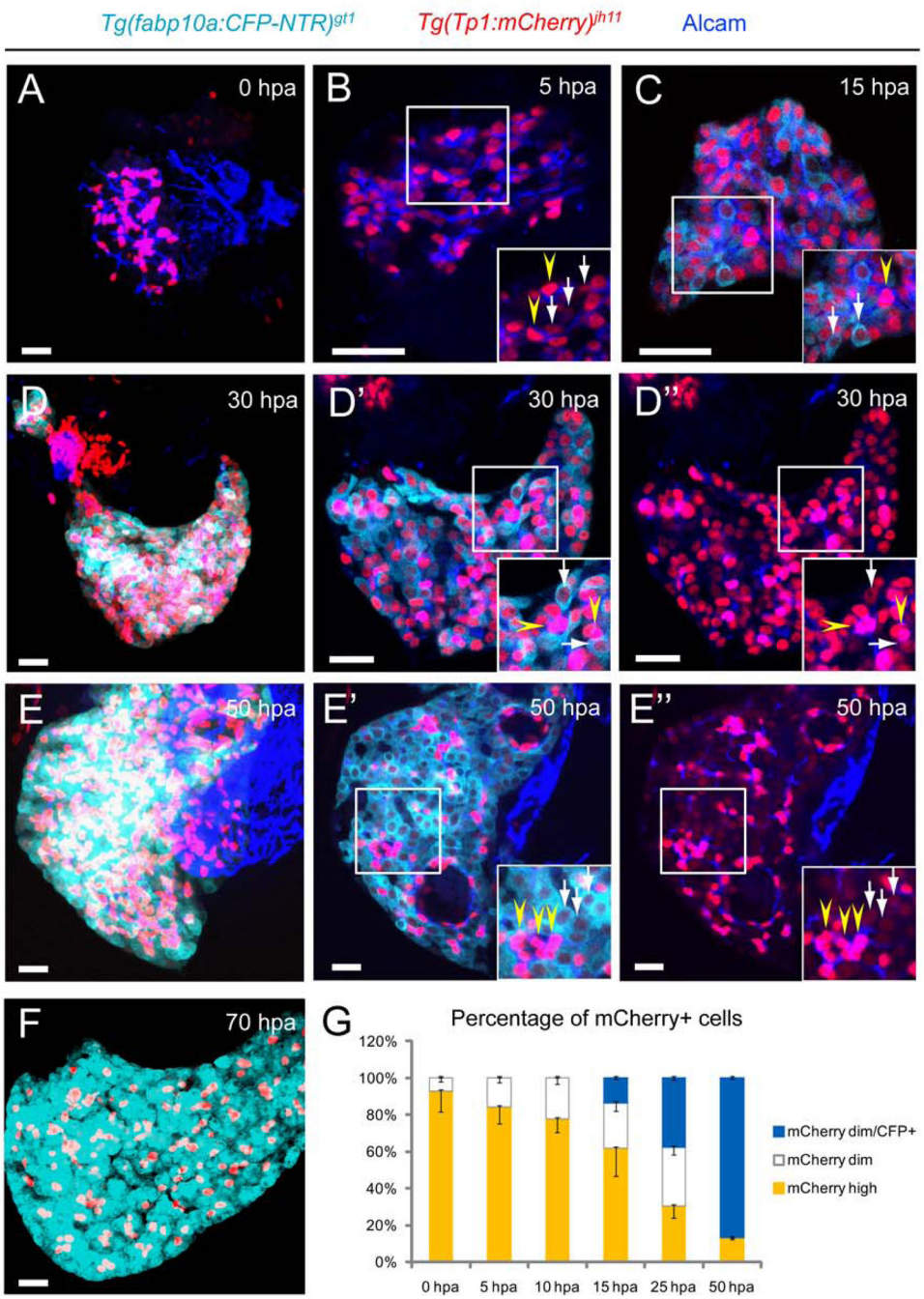

Fig. 3.

Heterogeneity of Notch signaling activity in the regenerating livers. (A–F) MTZ-treated larvae were collected at the indicated time points during liver regeneration. (A) NRCs marked by *Tg(Tp1:*mCherry) clustered together in close proximity at 0 hours-post-ablation (hpa). (B) The number of mCherry-expressing NRCs expanded at 5 hpa. Yellow arrowheads indicate bright red NRCs (inset), while white arrows indicate NRCs with dim red colors (inset). (C) At 13–15 hpa, hepatocyte-specific CFP started to co-express in a few dimming mCherry-positive NRCs throughout the regenerating livers (inset, white arrows), while the

bright red NRCs remained (inset, yellow arrowhead). (D–D") At 30 hpa, NRCs were clearly segregated into two heterogeneous populations, dim red NRCs co-expressing CFP (D', D", insets, white arrows) and bright red NRCs without CFP markers (D', D", insets, yellow arrowheads). (E–E") CFP-positive NRCs became CFP only-positive cells with the loss of red (E', E", insets, white arrows), continuing to increase in numbers at 50 hpa. Bright red NRCs remained as CFP-negative (E', E", insets, yellow arrowheads). (F) By 70 hpa, the conversion was nearly complete, resulting in the repopulation of the entire liver with newly generated hepatocytes. (G) Percentages (mean±SD) of dim red NRCs that contributed to newly formed CFP-positive hepatocytes in the first 50 hours of regeneration. At 15 hpa, hepatocyte-specific CFP began to emerge from the population of dim red NRCs (13.7±0.5% of dim red NRCs were CFP-positive). The percentage of dim red NRCs increased (0 hpa, 7.1±1.9%; 5 hpa, 15.9±2.6%; 10 hpa, 22.3±3.5%; 15 hpa, 37.7±4.6%; 25 hpa, 69.8±5.4%; 50 hpa, 87±0.7%) during the regeneration with all of the CFP-positive hepatocytes being derived from these cells (15 hpa, 13.7±0.5%; 25 hpa, 37.7±1.3%; 50 hpa, 87±0.7%). Cells in 5 planes of confocal images from 5 individual larvae were counted at each time point. All images are confocal single-plane images except A, D, E and F, which are projections images (n=30 larvae per each time point in three experiments). Scale bars, 20μm.

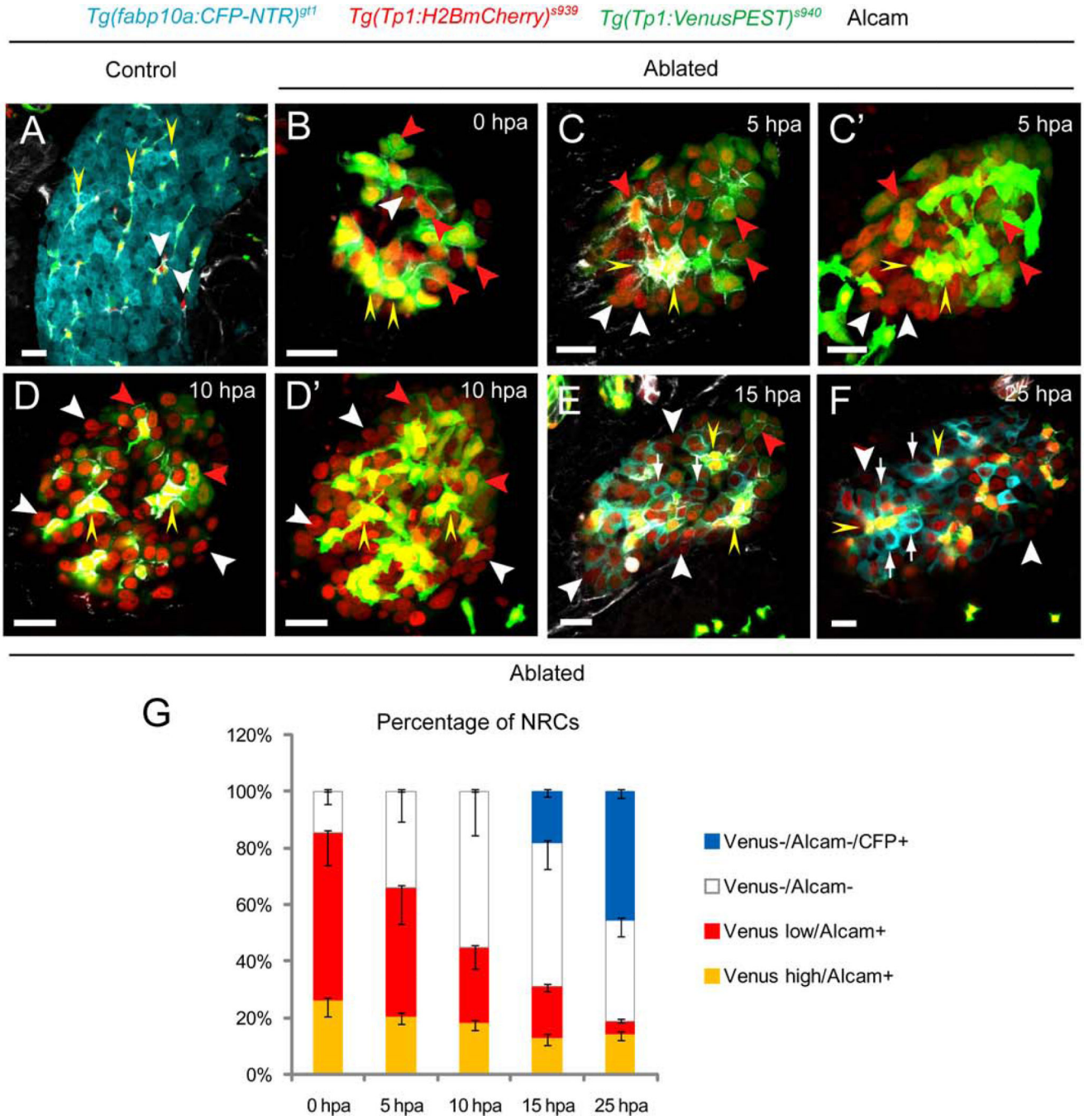

Fig. 4.

Distinct levels of Notch signaling are essential for the differentiation of the HPCs into hepatocytes. (A) In [*Tg(fabp10a:CFP-NTR)*^{gt1}*; Tg(Tp:H2BmCherry)*^{s939}*; Tg(Tp1:VenusPEST)*^{s940}] larvae treated with DMSO at 5 dpf, expression of *Tg(Tp1:*H2BmCherry) largely overlapped with that of *Tg(Tp1:*VenusPEST) (yellow arrowheads). A few *Tg(Tp1:*H2BmCherry)-single positive cells were observed (white arrowheads). (B–F) MTZ-treated larvae were collected at the indicated time points during liver regeneration. (B) At 0 hpa, *Tg(Tp1:*H2BmCherry)-positive NRCs were segregated into

*Tg(Tp1:*VenusPEST)$^{-}$/Alcam^{-} (white arrowhead), *Tg(Tp1:*VenusPEST)^{low}/Alcam^{+} (red arrowheads), and *Tg(Tp1:*VenusPEST)^{high}/Alcam^{+} (yellow arrowheads) group based on the intensity of Venus and Alcam expression. (C–D') The proportion of *Tg(Tp1:*VenusPEST)$^{-}$/Alcam cells^{-} (white arrowheads) started increasing significantly in the MTZ-treated regenerating livers with a decrease in *Tg(Tp1:*VenusPEST)^{low}/Alcam^{+} cells (red arrowheads) at 5–10 hpa. (E, F) At 15 hpa, all the converting CFP-positive NRCs (white arrows) were *Tg(Tp1:*VenusPEST)$^{-}$/Alcam^{-} cells with near absence of *Tg(Tp1:*VenusPEST)^{low}/Alcam^{+} cells at 25 hpa. Therefore, the *Tg(Tp1:*VenusPEST)^{low}/Alcam^{+} (red arrowheads) and *Tg(Tp1:*VenusPEST)$^{-}$/Alcam^{-} (white arrowheads) cells experiencing discrete levels of Notch downregulation at early stages of liver regeneration may equate to the transitioning HPCs. (G) Percentage (mean±SD) of *Tg(Tp1:*VenusPEST)$^{-}$/Alcam^{-} (0 hpa, 14.8±4.3%; 5 hpa, 34.0±10.6%; 10 hpa, 55.2±15.5%; 15 hpa, 69.1±11.0%; 25 hpa, 81.2±7.5%), *Tg(Tp1:*VenusPEST)^{low}/Alcam^{+} (0 hpa, 58.9±11.4%; 5 hpa, 45.3±12.7%; 10 hpa, 26.4±7.5%; 15 hpa, 17.7±1.7%; 25 hpa, 4.5±0.6%), *Tg(Tp1:*VenusPEST)^{high}/Alcam^{+} (0 hpa, 26.3±5.6%; 5 hpa, 20.7±2.8%; 10 hpa, 18.4±2.9%; 15 hpa, 13.2±2.8%; 25 hpa, 14.3±2.1%), and *Tg(Tp1:*VenusPEST)$^{-}$/Alcam/CFP^{+} cells (15 hpa, 18.3±1.8%; 25 hpa, 45.7±2.1%) during hepatocyte regeneration. Cells in 5 planes of confocal images from 5 individual larvae were counted at each time point. All images are confocal single-plane images except C' and D', which are projection images (n=30 larvae per each time point in three experiments). Scale bars, 20μm. SD, standard deviation.

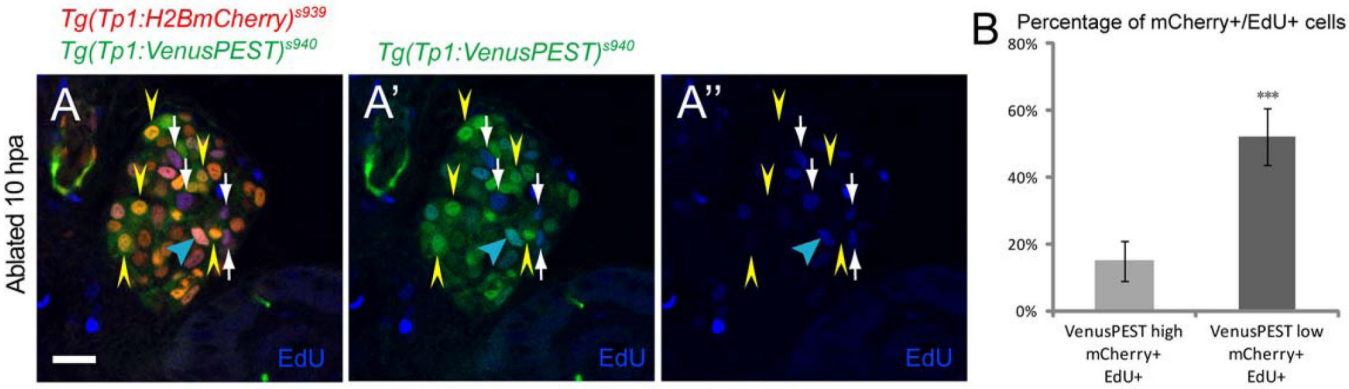

Fig. 5.

Distinct levels of Notch signaling are essential for the proliferation of the HPCs. (A–A") EdU incorporation in the MTZ-treated regenerating [*Tg(Tp1:H2BmCherry)*^{s939}*; Tg(Tp1:VenusPEST)*^{s940}] livers at 10 hpa. Confocal single-plane images showing more pronounced increase of an EdU incorporation in the NRCs with lower levels of *Tg(Tp1:*VenusPEST) expression (white arrows) than in higher levels (yellow arrowheads) with a few exceptions (blue arrowhead). (B) Percentages (mean±SD) of NRCs that incorporated EdU in the first 10 hours of regeneration. 52±8.5% of NRCs with lower levels of *Tg(Tp1:*VenusPEST) expression were EdU-positive, whereas 15±6.2% of NRCs with higher levels of *Tg(Tp1:*VenusPEST) expression were EdU-positive (500 cells counted in 10 larvae). Therefore, the population of NRCs with lower levels of *Tg(Tp1:*VenusPEST) expression and higher EdU incorporation may equate to the HPCs. Asterisks indicate statistical significance: ***p<0.001. All images are confocal single-plane images (n=30 larvae per each time point in three experiments). Scale bar, 20μm. SD, standard deviation.

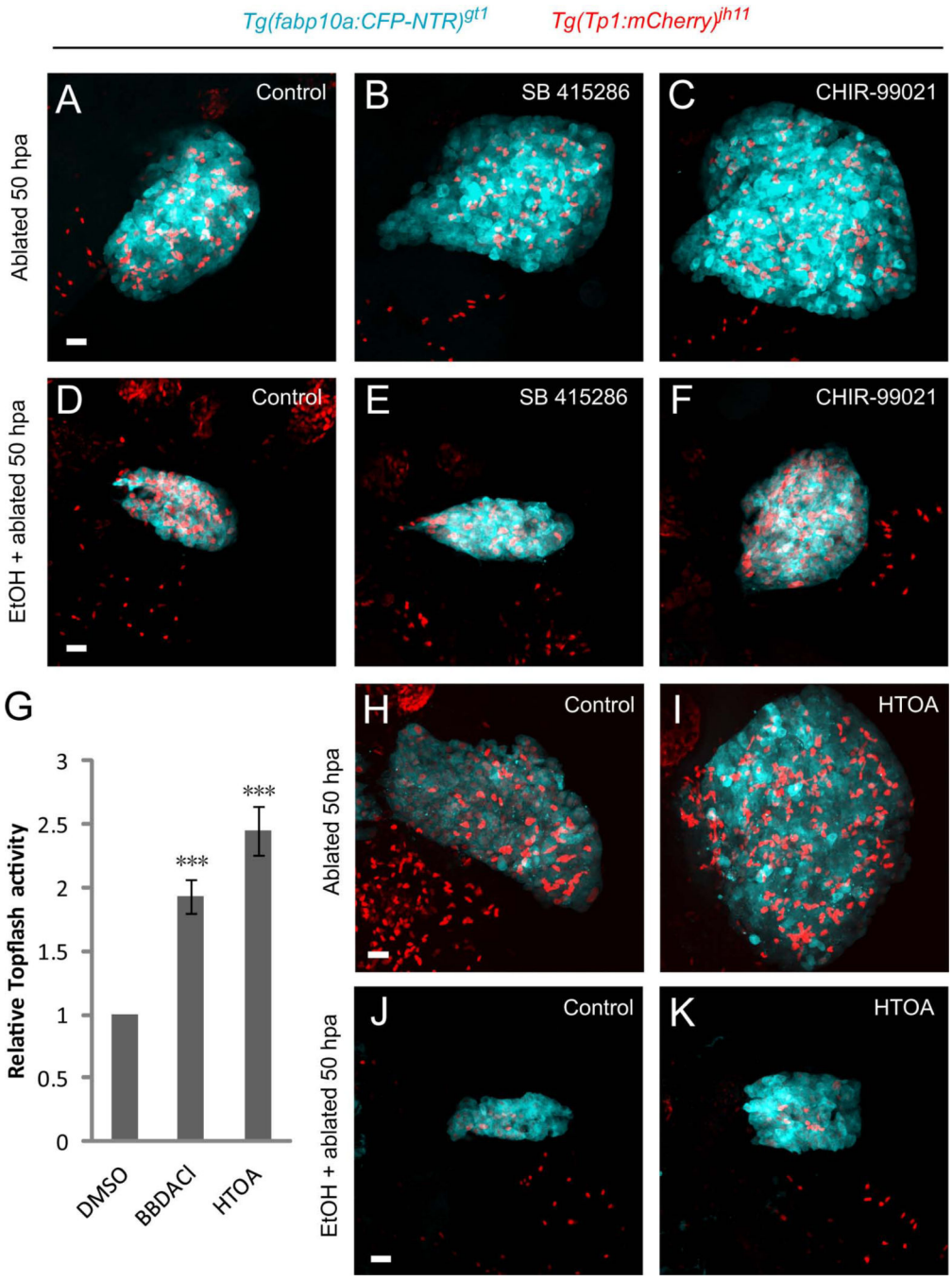

Fig. 6.

Chemical screens reveal the critical role of Wnt signaling in hepatocyte regeneration in the presence of sustained fibrogenic stimulus. (A–C) Wnt agonists promoted hepatocyte regeneration. Compared with the DMSO treatment (A), Glycogen synthase kinase-3 inhibitors SB415286 (B) and CHIR-99021 (C) increased hepatocyte regeneration. (D–F) In the EtOH/MTZ-treated regenerating livers, SB415286 (E) and CHIR-99021 (F) treatment augmented hepatocyte regeneration compared with that in the DMSO treatment (D). (G–K) Screen of a bioactive compound library. (G) Wnt activity reporter assay identifying

[bisbenzyldimethylamine, chloride] and [4-(1H-1,2,3,4-tetraazol-5-yl)-1,2,5-oxadiazole-3-ylamine], abbreviated as BBDACl and HTOA, respectively, as novel Wnt pathway activators. TOPflash reporter activity is presented as fold induction relative to the DMSO-treated controls. Fold increase was 1.93±0.14 and 2.45±0.19, respectively (n=4 experiments). Asterisks indicate statistical significance: ***$p<0.001$. (H–K) Confocal images showing HTOA treatment enhanced hepatocyte regeneration both in the MTZ- (I) and EtOH/MTZ- (K) treated regenerating livers compared to the respective DMSO treatment (H, J). All images are confocal projection images (n=30 larvae per condition in three experiments). Scale bars, 20μm. EtOH, ethanol.

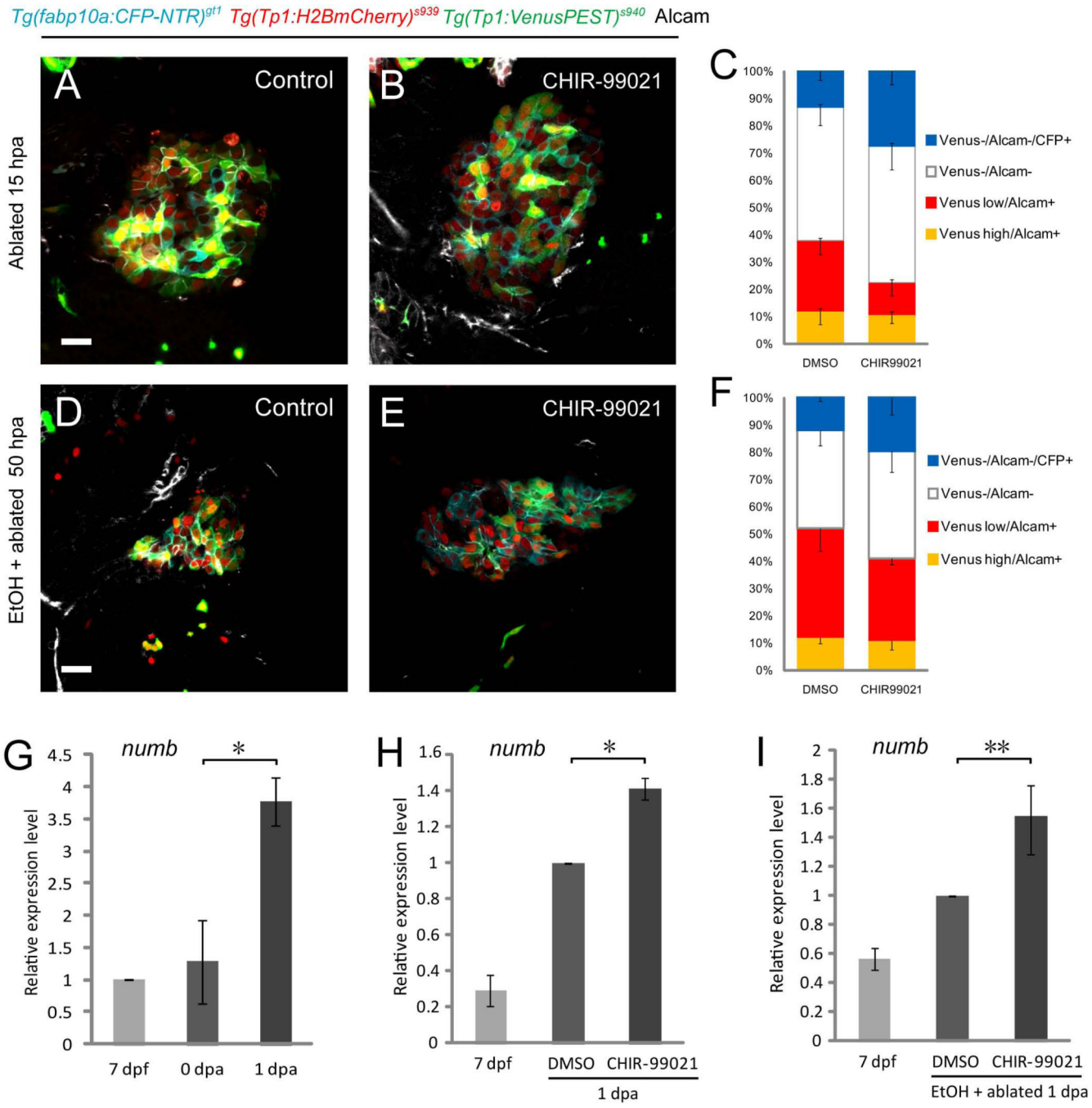

Fig. 7.

Wnt signaling antagonizes Notch signaling to promote hepatocyte regeneration in the presence of sustained fibrogenic stimulus. (A–F) Compared with the DMSO treatment (A, D), Wnt agonist CHIR-99021 increased the CFP^+ cells while downregulating *Tg(Tp1:*VenusPEST) expression both in the MTZ- (B) and EtOH/MTZ- (E) treated regenerating livers. (C, F) Comparison of the percentage of $Tg(Tp1{:}VenusPEST)^{high}/Alcam^+$ (MTZ/DMSO, 12.0±4.9%; MTZ/CHIR99021, 10.7±3.2%; EtOH/MTZ/DMSO, 12.0±2.2%; EtOH/MTZ/CHIR99021, 10.8±3.2%), $Tg(Tp1{:}VenusPEST)^{low}/Alcam^+$(MTZ/

DMSO, 25.7±5.2%; MTZ/CHIR99021, 11.8±4.7%; EtOH/MTZ/DMSO, 40±8.3%; EtOH/MTZ/CHIR99021, 30.2±2.3%), *Tg(Tp1:*VenusPEST)$^{-}$/Alcam^{-} (MTZ/DMSO, 62.3±9.9%; MTZ/CHIR99021, 77.5±13.6%; EtOH/MTZ/DMSO, 48.0±6.8%; EtOH/MTZ/CHIR99021, 59.0±13.8%), and *Tg(Tp1:*VenusPEST)$^{-}$/Alcam^{-}/CFP^{+} cells (MTZ/DMSO, 13.2±3.2%; MTZ/CHIR99021, 27.5±5.0%; EtOH/MTZ/DMSO, 12.0±1.2%; EtOH/MTZ/CHIR99021, 19.7±6.2%) between the DMSO- vs. Wnt agonist-treated regenerating livers. Wnt agonist treatment significantly increased the total percentage of CFP-positive hepatocytes and *Tg(Tp1:*VenusPEST)$^{-}$/Alcam- cells, in which all CFP-positive hepatocytes were derived from, with a decrease in *Tg(Tp1:*VenusPEST)^{low}/Alcam^{+} cells both in the MTZ- (C) and EtOH/MTZ- (F) treated regenerating livers. Cells in 5 planes of confocal images from 5 individual larvae were counted. (G) qRT-PCR analysis of *numb* mRNA in control (7 dpf), MTZ-treated (0 dpa) and MTZ-treated regenerating livers (1 dpa). *numb* was significantly upregulated in the 1 dpa MTZ-treated regenerating livers. (H, I) Wnt agonist CHIR-99021 upregulated *numb* expression both in the MTZ- (H) and EtOH/MTZ- (I) treated regenerating livers. n=150 dissected larval livers per condition in three experiments. Asterisks indicate statistical significance: *p<0.05 and **p<0.01. All images are confocal single-plane images (A, B, n=30 larvae per condition in three experiments; D, E, n=15 larvae per condition in three experiments). Scale bars, 20μm. EtOH, ethanol; SD, standard deviation.

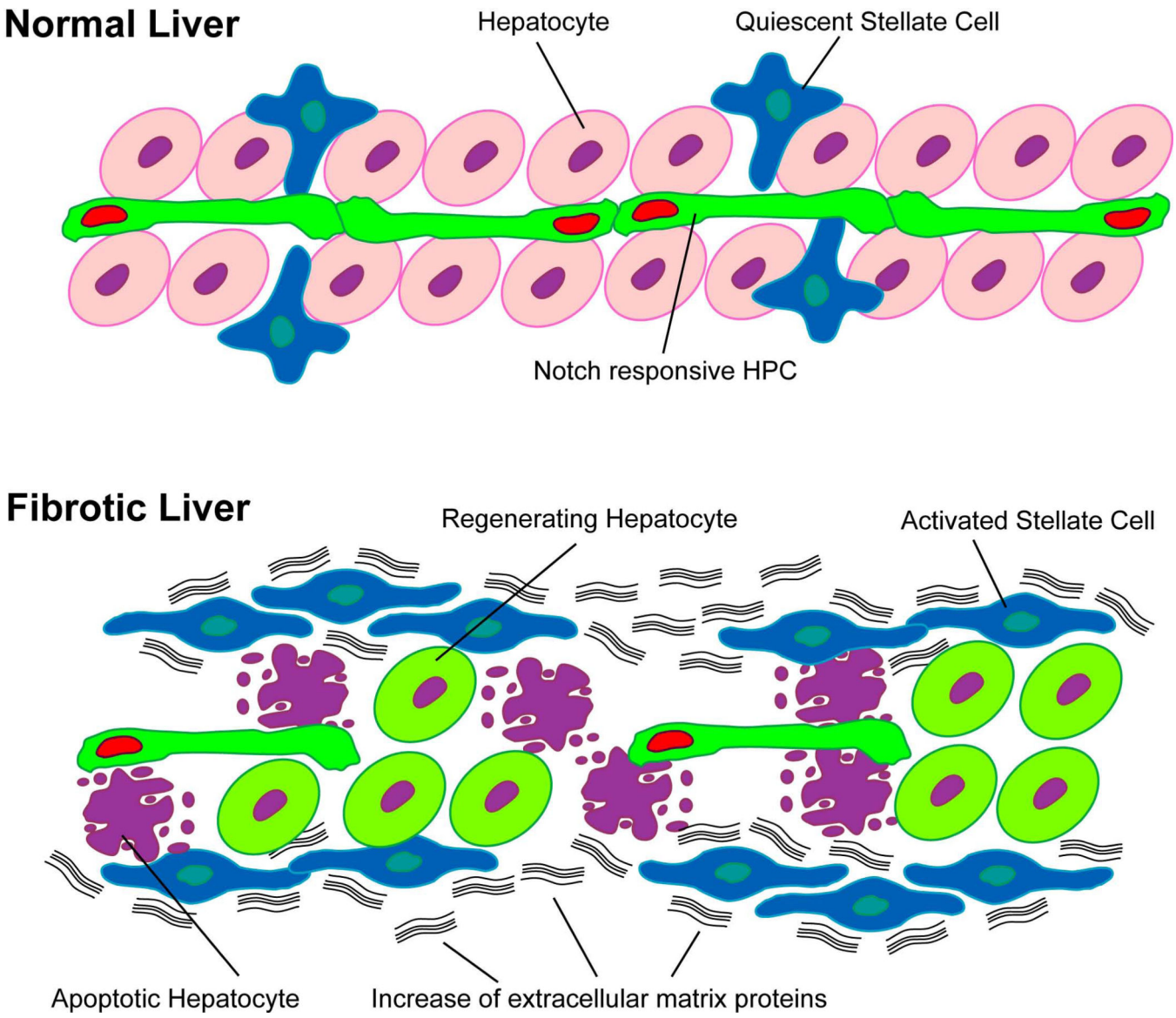

Fig. 8.

Notch responsive HPCs retain their capacity to regenerate as hepatocytes in the presence of sustained fibrogenic stimulus. In the normal liver, both the Notch responsive hepatic progenitor cells (HPCs, green cells with red nuclei) and the hepatic stellate cells (HSCs, blue cells with star-like configuration) are quiescent. In the presence of sustained fibrogenic insult, activation of HSCs (blue cells lose star-like configuration) leads to an increase in both their numbers and production of the extracellular matrix (ECM) proteins (black wavy lines). Induction of near-complete destruction of hepatocytes (purple cells with blebbings) in this setting stimulates the activation of the HPCs, resulting in the downregulation of the Notch signaling in these cells for proliferation and subsequent differentiation to hepatocytes (light green cells with purple nuclei).